# Active Magnetic Bearings for 10kWh Flywheel Energy Storage System

Osamu Saito, Soichiro Une, Hisayuki Motoi
Ishikawajima-Harima Heavy Industries Co.,Ltd
1-15,Toyosu 3 chome, Koto-ku, Tokyo 135-8732, Japan

Hironori Kameno , Yasukata Miyagawa , Ryouichi Takahata , Hirochika Ueyama
R&D Center, KOYO SEIKO CO., LTD.
No.333, Toichi-chou, Kashihara, Nara 634-0008, Japan

## SUMMARY

As the demand for electric power has been increasing steadily, a flywheel energy storage system (FESS) using magnetic bearings is needed in order to level daily load of electric power. We have succeeded to suspend a flywheel of 385kg in total weight which has a 1,000mm diameter carbon fiber reinforced plastics (CFRP) rotor performing as 10kWh FESS by means of 5 axis controlled active magnetic bearings ( A.M.B.).

This paper presents the A.M.B. used in the above system controlled by digital signal processor (DSP). The switching power amplifiers of the A.M.B. can supply maximum current of 8A per channel driven by 300V supply voltage. The radial electromagnets were designed as so called homopolar type in order to reduce rotational loss due to eddy current. The decentralized controller was designed for upper and lower radial bearings using bias current system linearization. On the other hand, an axial electromagnet was designed as a permanent magnet biased (non-linear) actuator.

It is possible not only to monitor the displacement of the rotor and control currents in the electromagnet but also to change control parameters of each axis from personal computer by means of serial communication, including telephone line with modem, accessing directly to the DSP.

The paper also reports the system information of the FESS and measured data during stand still and rotation by means of above mentioned serial communication.

## INTRODUCTION

In a flywheel energy storage system (FESS) , the electric energy is stored as the kinetic energy of the rotating flywheel and it is taken out as electric energy if needed. In past studies, it had been considered that it was difficult to supply the energy more than one hour because the rotational loss of ball bearing was very large. Furthermore, there was no suitable material for flywheel which has high tensile strength against its density.

By the way, there were only a few reports about the flywheel rotor supported by contact free A.M.B. which can be accelerated up to a certain high speed practically. One of the reasons seems to be that it is very difficult to control and stabilize the natural frequency vibration of the rotor by A.M.B. Additionally, large gyro effect due to large moment of inertia around rotational axis increase such difficulties.

Recently, it was revealed that a high-Tc superconductor ($YBa_2Cu_3O_{7-x}$) which has a strong pinning force was used in magnetic bearings [1] and the rotational loss of superconducting magnetic bearings was very small [2]. In these conditions, it is expected that the superconducting magnetic bearings could be used for large scale FESS. Also, the development of CFRP for FESS rotor has advanced remarkably.

In Japan, a national research and development project of FESS using superconducting magnetic bearings was started in 1995. In this project, a small type model of 0.5kWh class FESS system was assembled, tested and discussed about its rotor dynamics in 1998 [3]. Currently, as a further step, a middle type model of 10kWh class FESS which rotor was suspended by A.M.B. (without superconducting magnetic bearing) has been tested in order to verify the developed know how in rotor dynamics for FESS.

## STRUCTURE OF FESS ROTOR

Figure 1 shows a structure of 10kWh flywheel system and Table 1 shows a specification of the system respectively. It is necessary to place the rotor and bearings in a vacuum housing in order to minimize aerodynamic drag (windage loss). A flywheel (FW) made of carbon fiber reinforced plastic (CFRP) was shrunk-fitted to an aluminum hub connected on a main hollow shaft. A synchronous motor rotor was installed in the inside of main hollow shaft in order to perform energy input (acceleration) and output (deceleration). Two lamination cartridges of radial rotor core made by silicon steel plate for the radial active magnetic bearings (RaAMB) were also shrunk-fit to each end of the main shaft. In addition, a ring shaped disk for the axial active magnetic bearings (AxAMB) was attached to the upper end of the main shaft. The rotor assembly was levitated by RaAMB and AxAMB without mechanical contact in all directions. When the radial/axial vibration or displacement exceeds the control limit of the A.M.B.s, the main shaft touches the inner race of the emergency ball bearings in order to prevent

the rotor from being damaged. For future study in this project, it is possible to install permanent magnet in the inner side of main hollow shaft rotor for radial type superconducting magnetic bearings[4].

## DESIGN OF ACTIVE MAGNETIC BEARINGS

The electromagnets of RaAMBs are homo-polar type in order to reduce drag torque due to eddy current loss in the radial rotor core. Table 2 shows the specification of A.M.B.s for this system.

The RaAMBs and AxAMB are totally controlled by Digital Signal Processor (DSP) TMS320C50. Thanks to the digitally controlled system, it is possible to monitor the displacement of the rotor and current of the A.M.B.s from a personal computer through serial communication. The autonomous scheduled diagnosis including residual unbalance of the rotor, running orbit analysis, etc are easily implemented by monitor software. Using modem and a telephone line as shown figure 2, it is also possible to access to the A.M.B. controller from any long distance place. (ex. From Santa Barbara to Tokyo). The PWM (Pulse Width Modulation) switching power amplifiers of the A.M.B.s, which switching frequency is 100KHz, can supply maximum peak current of 8A per channel driven by 300V supply voltage. The inductance type displacement sensors for radial direction are used and eddy current type displacement sensor are used for axial direction.

## ANALYSIS OF ROTOR DYNAMICS

The entire rotor assembly consisting of shaft, hub and FW, as shown Figure 3, was modeled by means of the Finite Element Method (FEM). Finally a State-Space expression was used for mathematical rotor model which is easily used for total system analysis including feedback structure of A.M.B.s.

Figure 4 (a) shows a modeled entire rotor assembly used in this analysis. As a result, first 3 natural frequencies and corresponding bending mode shape at stand still were calculated as shown in figure 4 (b),(c) and (d). Figure 4 (b) and (c) show 1st and 2nd bending mode mainly due to the deformation of hub and FW. Contrary, figure 4(d) shows 3rd bending mode of rotor, which is resulted from 1st bending mode of main shaft. In the above natural frequency analysis, RaAMBs were expressed as simple spring element.

Figure 5 shows analysis results of natural frequencies of first 2 rigid mode of 1R, 2R,and above mentioned 1B,2B and 3B including frequency response of upper and lower RaAMBs. The natural frequency of the rigid mode are results from the characteristics of RaAMB (resonance of A.M.B. stiffness and mass, rotating moment of inertia of the rotor) and 1B,2B,3B show natural frequency of bending mode caused by the elasticity of the rotor. It is indicated that each natural

frequency value is split in two branches (forward and backward) by increase of the rotational speed due to gyroscopic effect. The rotor speed is shown as a straight line in figure 5. At intersection of each natural frequencies and the line, the rotor can be expected to vibrate by resonance (critical speed). For accelerating the rotor at system target speed of 17,200rpm, the rotor has to pass through resonant frequency of backward 1B at 12,500rpm after passing resonant frequencies of 1R,2R. The controller of the RaAMBs has to be designed to stabilize these vibration mode and to pass the critical speed.

## RESULT OF ROTATIONAL TEST

After the rotor was successfully suspended by AMB, the dynamic stiffness could be measured indirectly as the reciprocal of the sensitivity transfer function of the controller which has the input of the disturbance force to the rotor and output of the displacement of the rotor. These measurements can be easily carried out by developed built-in function of DSP. Figure 7 shows the dynamic stiffness measured in upper and lower RaAMB and AxAMB. Measured values of natural frequencies were nearly equal to calculated values in figure 4. The 3B bending mode was not found clearly in measured data, because this mode was thought to be damped quite well.

The rotor was accelerated up to 8,000rpm in this step. The actual natural frequencies were obtained from dynamic stiffness data measured during rotation. Figure 6 shows the measured results of interesting natural frequencies. The branch of measured 1B was larger than that of calculated value. But except for it, the whole branch of measured natural frequencies were predicted well by that of calculated results.

Figure 8 shows the results of measured run-out (orbit) in radial direction and axial direction at 8,000rpm. The run-out was approximately less than 5_m and the rotor vibration were damped well by RaAMBs. The rotor will be accelerated up to the target speed of 17,200rpm in near future.

## CONCLUSIONS

The prototype of 10kWh class flywheel energy storage system which has the flywheel rotor of diameter 1,000mm and rotor weight of 385kg was supported by the Active Magnetic Bearings without mechanical contact. The whole rotor assembly could be successfully accelerated up to 8,000rpm. As a result, kinetic energy of the system was achieved about 2kWh. This energy storage value will became larger in near future by reaching more higher speed step by step, and will be finally achieved 10kWh at 17,200rpm.

In this study, the rotor dynamics of the flywheel energy storage system whose rotor had large gyroscopic effect including RaAMB dynamics were analyzed in detail, and the rotor vibration due to natural frequencies was damped well by RaAMBs.

This study was funded by the New Energy and Industrial Technology Development Organization (NEDO) in Japan, as a part of the Japanese national project "High-Temperature Superconducting Flywheel Energy Storage System."

## REFERENCES

[1] R.Takahata, H.Higasa, H.Ueyama, Y.Miyagawa, H.Kameno and F.Ishikawa ; "Trial Manufacturing of 0.2kWh Class Flywheel Rotor Supported by superconducting Magnetic Bearing, T.IEE, Vol.117-D, No.9, 1132_1138(1997) in Japanese

[2] H.J.Bornemann, T.Ritter, C.Urban, O,Zaitsev, K. Weber and H.Rietschel _ "Low Friction in A Flywheel System with Passive Superconducting Magnetic Bearings", Applied Superconductivity Vol.2,No.7/8,439_447(1994)

[3] Y.Miyagawa, H.Kameno R.Takahata, and H.Ueyama; "A 0.5kWh Flywheel Energy Storage System using A High-Tc Superconducting Magnetic bearing", IEEE Transaction on Applied Superconductivity, Vol..9, No.2 996_999(1999)

[4] H.Kameno Y.Miyagawa, R.Takahata, and H.Ueyama; "A Measurement of Rotation Loss Characteristics of High-Tc Superconducting Magnetic bearing and Active Magnetic bearings", IEEE Transaction on Applied Superconductivity, Vol..9, No.2 972_975(1999)

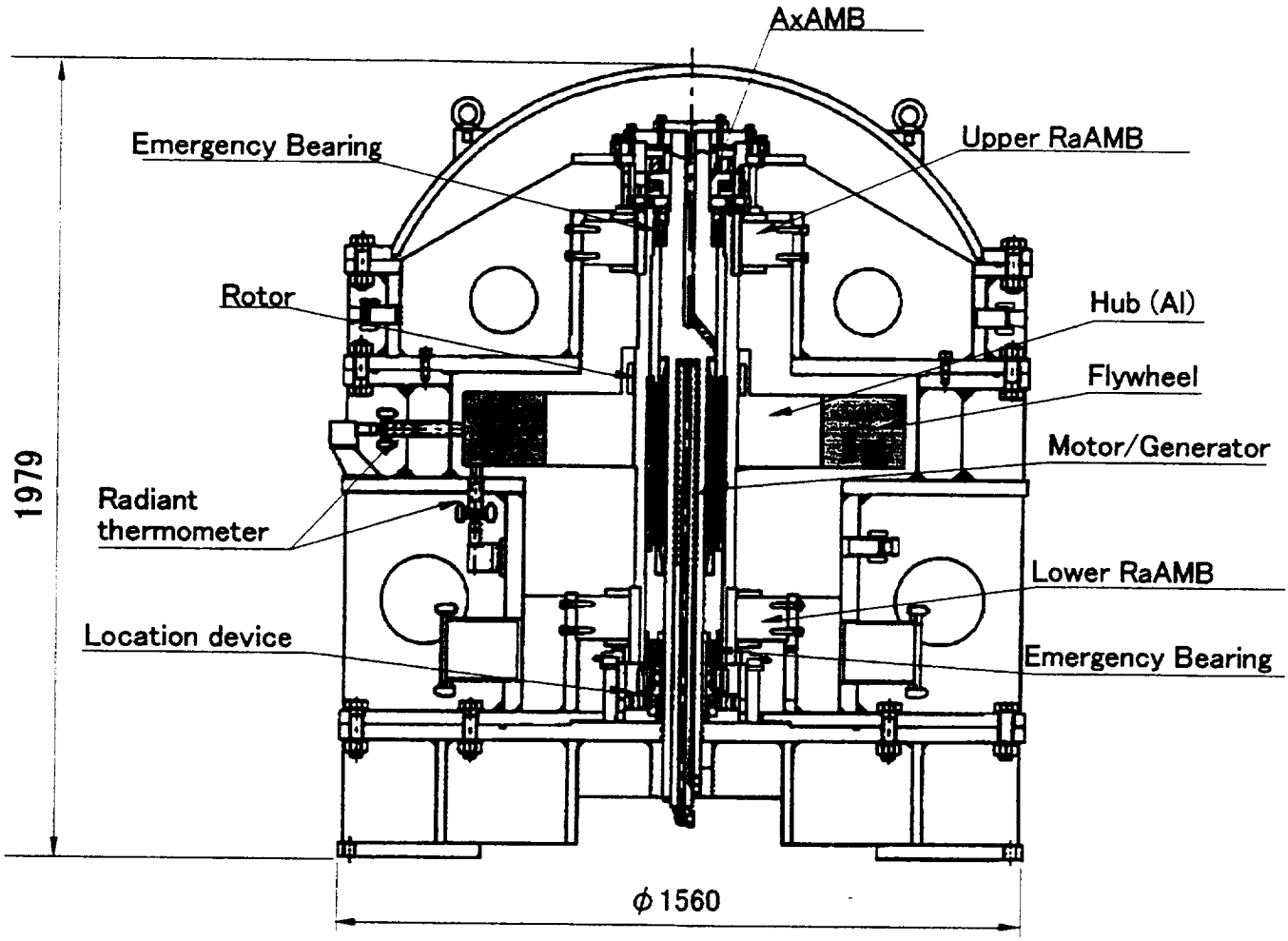


Figure 1 Structure of 10kWh flywheel system

Table 1 Characteristics of 10kWh flywheel system

| | |
|---|---|
| Pressure | Less than 0.14 Pa<br>(0.001 Torr) |
| Storage Energy | 10kWh ( at 17,200rpm) |
| Rotation Speed | 17,200 rpm ( target)<br>8,000rpm ( achievement) |
| Inertia moment | $2.79\times10^{8}$gcm$^{2}$ |
| Length of Rotor | 1,060 mm |
| Mass of Rotor | 385 kg |
| Flywheel | CFRP<br>$\phi$ 1000× $\phi$ 625×165 |
| Motor／Generator | Synchronous type 2kW |

Table 2 Data of Active Magnetic Bearings

| | |
|---|---|
| Control method | Digital control |
| Bias Current of RaAMB | 1.5 A |
| Bias Current of AxAMB | 3.0A |
| Air gap at AxAMB | 0.4mm (axial direction) |
| Air gap at RaAMB | 0.4mm (radial direction) |
| Air gap at emegency bearing | 0.2mm (axial direction)<br>0.2mm (radial direction) |
| Type of electromagnet (RaAMB) | Homopolar type<br>Inner diameter : 240.8mm |
| Material of rotor (RaAMB) | Super-E core(NKK)<br>(0.1mm thick) |

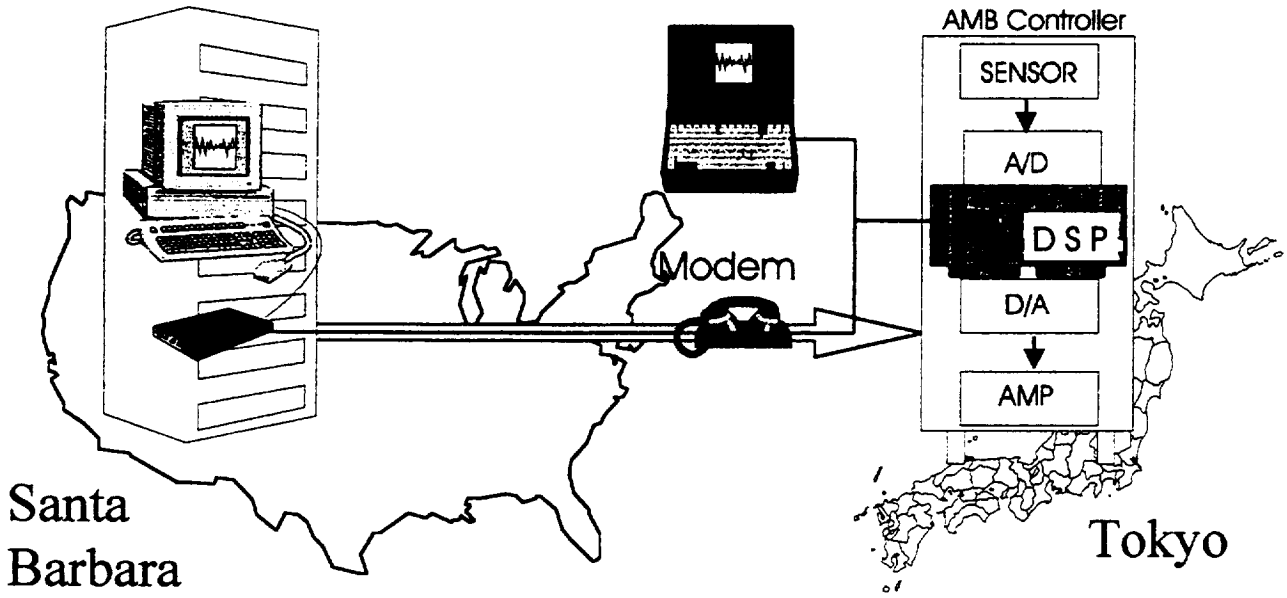


Figure 2 Remote control of AMB controller

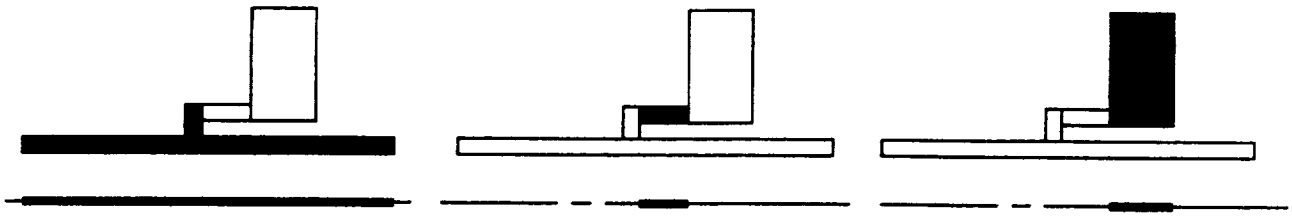

(a) Shaft (b) Hub (c) Flywheel(FW)

Figure 3 Modeling structure of the rotor consist of a shaft, hub and flywheel

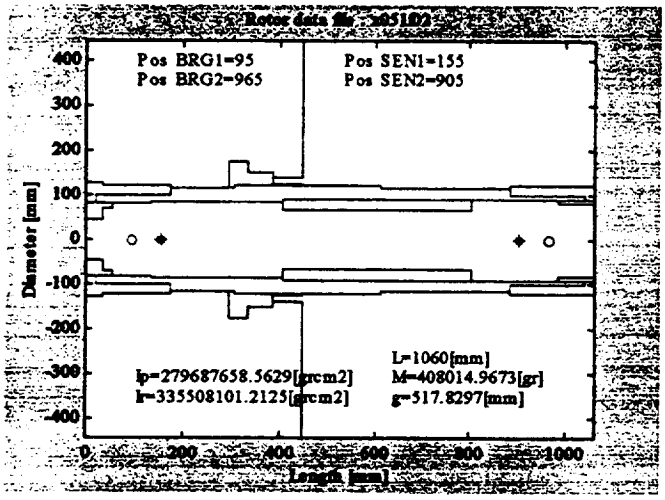


(a) Modeling structure of the rotor

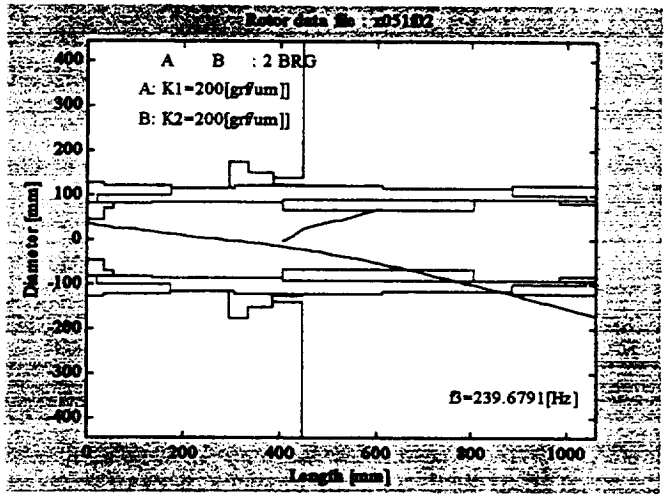


(b) 1st bending mode mainly due to hub and FW

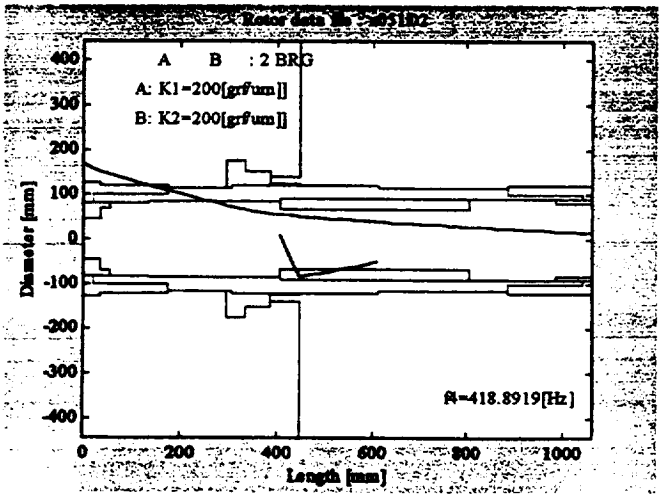


(c) 2nd bending mode mainly due to hub and FW

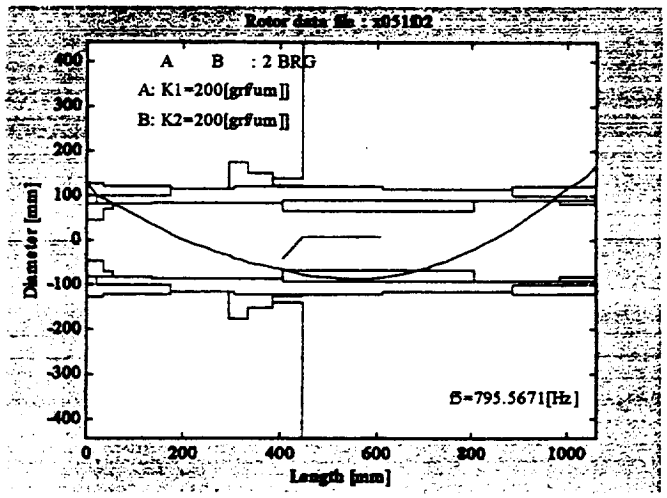


(d) 3rd bending mode mainly due to shaft

Figure 4 Analyzed results of natural frequency of the rotor

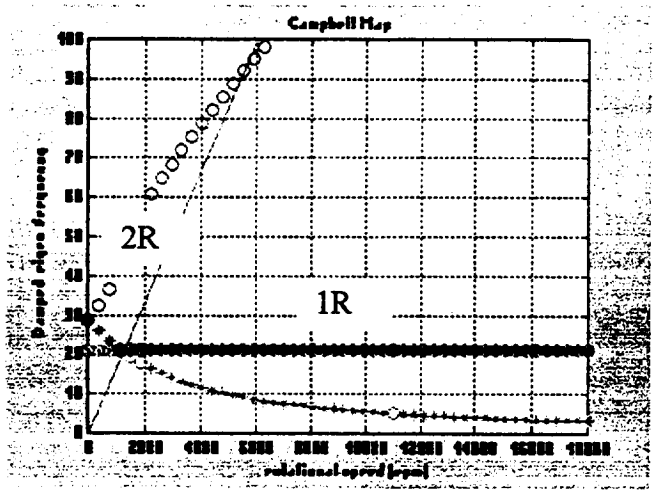


(a) 2 rigid mode natural frequency

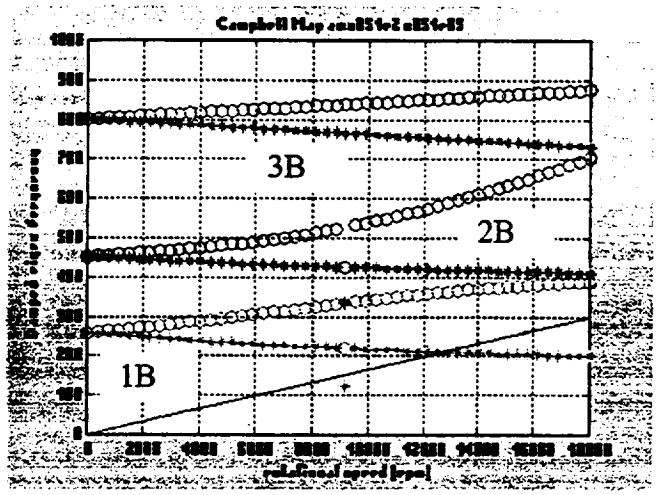


(b) 3 bending mode natural frequency

Figure 5 Analyzed results of natural frequency of the rotor

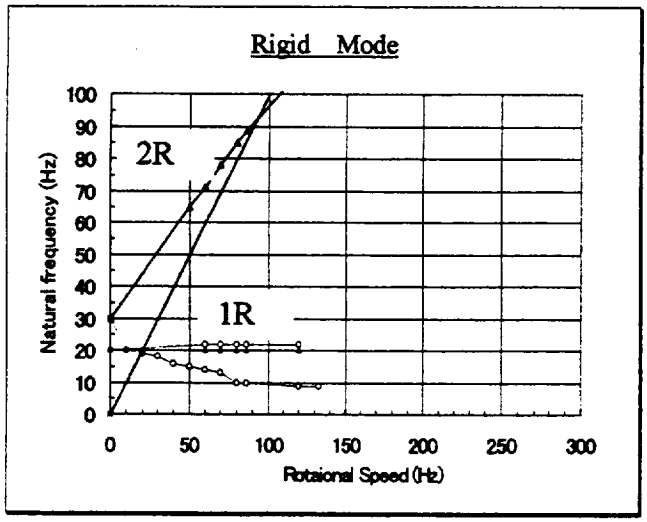


(a) 2 rigid mode natural frequency

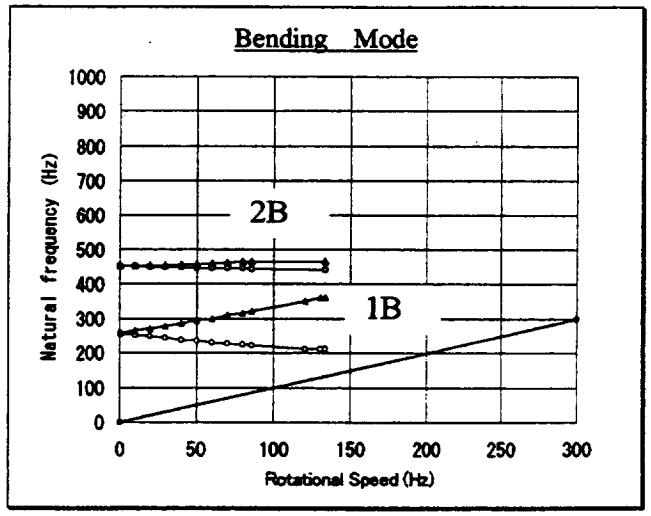


(b) 2 bending mode natural frequency

Figure 6 Measured results of natural frequency of the rotor

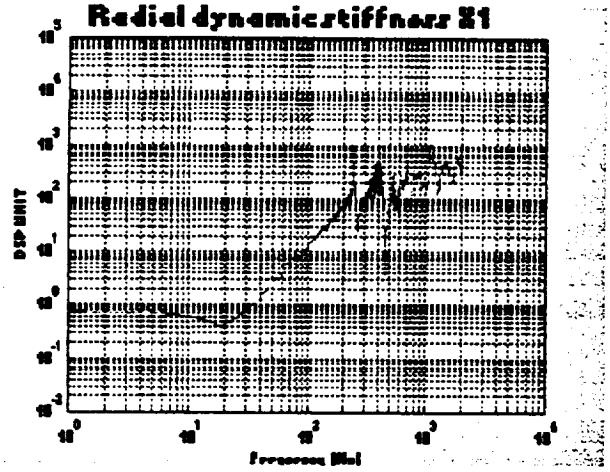


(a) Upper RaAMB portion

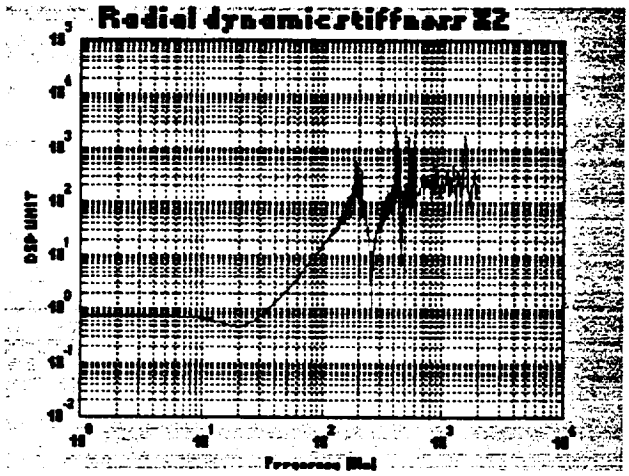


(b) Lower RaAMB portion

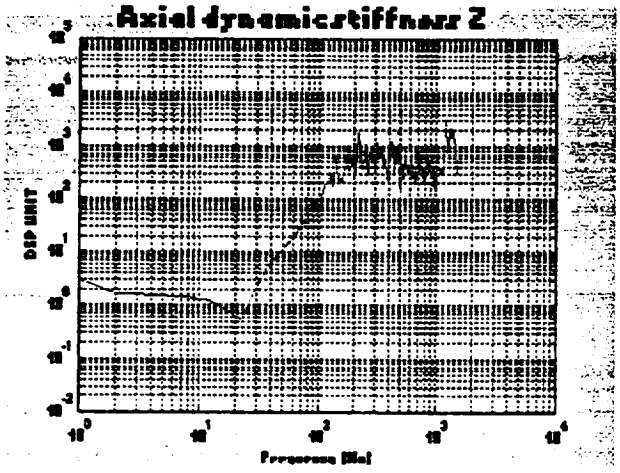


(c) AxAMB portion

Figure.7 Dynamic stiffness of each AMB(measured)

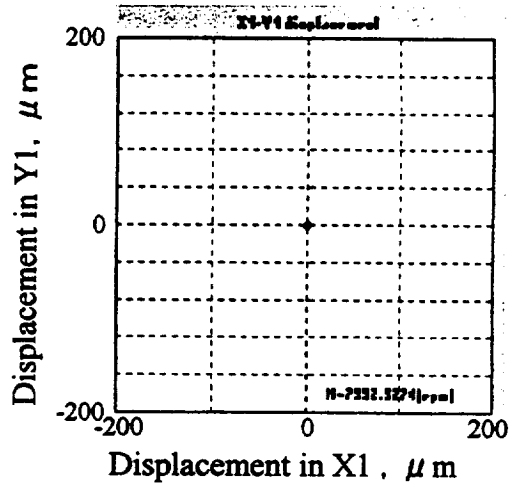


(a) Upper RaAMB portion

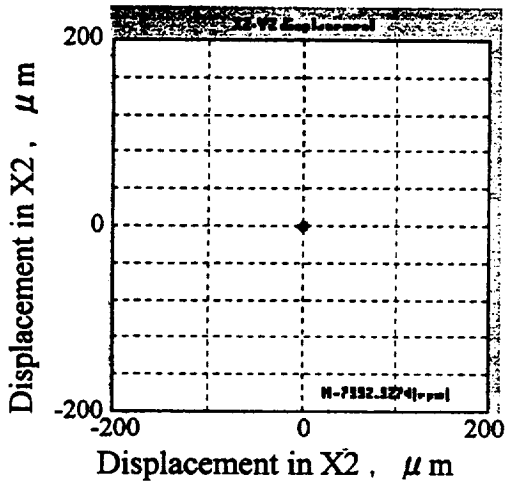


(b) Lower RaAMB portion

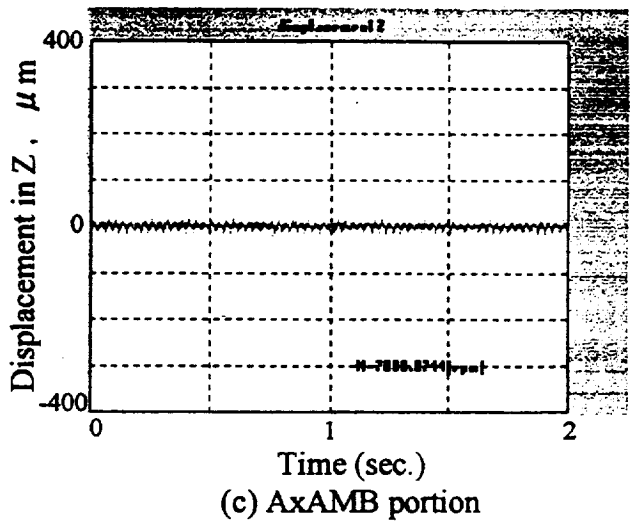


(c) AxAMB portion

Figure.8 runout of the rotor in each AMB portion